# Arbitrary Multiplication and Division of the Orbital Angular Momentum of Light

Yuanhui Wen,[1] Ioannis Chremmos,[2] Yujie Chen,[1,*] Yanfeng Zhang,[1] and Siyuan Yu[1,3,†]
[1]State Key Laboratory of Optoelectronic Materials and Technologies, School of Electronics and Information Technology, Sun Yat-sen University, Guangzhou 510275, China
[2]Hellenic Electricity Distribution Network Operator S. A., Athens 11743, Greece
[3]Photonics Group, Merchant Venturers School of Engineering, University of Bristol, Bristol BS8 1UB, United Kingdom

(Received 7 February 2020; accepted 13 May 2020; published 26 May 2020)

Multiplication and division of the orbital angular momentum (OAM) of light are important functions in the exploitation of the OAM mode space for such purposes as high-dimensional quantum information encoding and mode division multiplexed optical communications. These operations are possible with optical transformations that reshape optical wave fronts according to azimuthal scaling. However, schemes proposed thus far have been limited to OAM multiplication by integer factors and require complex beam-copying or multitransformation diffraction stages; a result of the limited phase excursion $2\pi\ell$ around the annulus of an OAM state $\exp(i\ell\theta)$. Based on the key idea that the phase excursion along spirals in the transverse plane of a vortex is theoretically unlimited, we propose and experimentally demonstrate a simple yet effective scheme using an azimuth-scaling spiral transformation that can accomplish both OAM multiplication and division by arbitrary rational factors in a single stage.

DOI: 10.1103/PhysRevLett.124.213901

Orbital angular momentum (OAM), as an essential property of light, has constantly attracted intensive attention since the realization that a paraxial light field with a spiral phase structure $\exp(i\ell\theta)$ carries a definite amount $\ell\hbar$ of OAM per photon [1], where $\theta$ is the azimuthal angle and integer $\ell$ is the topological charge. OAM of light not only enables particle trapping and rotating in optical manipulation [2,3], enhanced resolution in microscopy [4,5] and rotational Doppler shift in optical metrology [6,7], but additionally, it endows the photon with a new degree of freedom ($\ell$) with a theoretically unbounded state space, which can be exploited for various applications such as high-capacity optical communication [8–10], high-dimensional quantum entanglement [11] and quantum key distribution [12,13].

Precise generation, manipulation, and detection of OAM states are critical for OAM-based applications, with generation and detection having been widely investigated. The available techniques for generating OAM states include holograms [14], mode converters [15], spiral phase plates [16], spin to OAM conversion [17], and integrated vortex emitters [18], while techniques for simultaneously detecting different OAM states include Mach-Zehnder interferometers [19,20], algorithmically designed vortex gratings [21,22], integrated devices [23], time-resolved spectral mapping [24], multiplane spatial light modulation [25], and the simple yet effective optical geometrical transformations [26–29].

By contrast, challenges still remain in the transformation and manipulation of OAM states, which are especially required in both OAM-based optical communication systems [9,30–32] and high-dimensional quantum information systems [33] to realize complex switching and routing functions. One such scenario is the switching of the data encoded on a set of OAM modes (or channels) $\{\ell\}$ to the set of modes $\{n\ell\}$, with $n$ generally being rational. For example, assume that the OAM channels $\{\ell = 1, 2, \ldots, N\}$ in two optical fibers are to be multiplexed and transmitted in an interlaced fashion through the OAM channels $\{\ell = 1, 2, \ldots, 2N\}$ in a third fiber. This requires the operations $\{\ell\} \to \{2\ell\}$ and $\{\ell\} \to \{2\ell - 1\}$ on the modes in the first and the second fibers, respectively, so that they are converted to even-$\ell$ and odd-$\ell$ OAM modes in the third fiber. To demultiplex back to the original OAM sets, the inverse operations $\{\ell\} \to \{\ell/2\}$ and $\{\ell\} \to \{(\ell + 1)/2\}$ have to be applied, respectively, on the even-$\ell$ and odd-$\ell$ OAM modes in the third fiber which can be discriminated interferometrically [19]. Such operations may also be useful in optical data encoding to expand the code space by inserting redundant states into an otherwise continuous state space, e.g., to improve error resistance and enable error correction [34].

The aforementioned functions require the multiplication of the vortex charges of a set of integer OAM states $\{\ell\}$ with a common rational factor $n$. Being essentially functions between spatial coordinates rather than between fields, optical geometrical transformations [35] are particularly attractive for implementing $\ell$-independent OAM multiplication that can work for any number of OAM states, and two such transformations have been employed so far with certain complexities and limitations. The first transformation is the log-polar mapping that unfolds the

 

annular intensity profile of a vortex $\exp(i\ell\theta)$ into a rectangular profile with linear phase. Subsequently, a fan-out grating produces $n$ copies (for integer $|n| > 1$) of this plane-wave state in the form of an elongated rectangle with $n \times 2\pi\ell$ phase range. An inverse log-polar mapping finally folds this rectangle back to an annulus with phase $\exp(in\ell\theta)$ [36]. The scheme is power efficient, but the cascaded transformation stages add complexity to the experimental setup and sensitivity to practical misalignment. The second transformation is the circular-sector mapping which applies a direct azimuthal scaling $(\theta \to \theta/n)$ to the input OAM state. For integer $|n| > 1$, an annulus is mapped to an annular sector of angle $2\pi/n$. With $n$ such simultaneous transformations on the same phase mask, $n$ complementary sectors are produced and combined in a complete annulus with phase $\exp(in\ell\theta)$. This single-stage scheme has lower complexity, however at the cost of power loss due to complex amplitude modulation [37] or higher-order diffraction [38] by the multitransformation phase mask [39]. Moreover, both the above schemes are limited to OAM multiplication by integer factors and need a different treatment for OAM division ($|n| < 1$) [38,40,41].

An inherent limitation of the above schemes is that the basic geometrical shape being transformed, namely the intensity annulus of an OAM state $\exp(i\ell\theta)$, restricts the azimuthal variable to a $2\pi$ range and, consequently, the available phase range to $2\pi\ell$. As a result, complex beam-copying or multitransformation diffractive stages have to be designed in order to accomplish the desired $n$-fold multiplication of the phase.

In this Letter, we propose a simpler yet effective single-stage scheme which achieves both OAM *multiplication* and *division* by an *arbitrary rational* factor $n$. The scheme is inspired by the recently introduced spiral transformation for high-resolution OAM mode sorting [28,29], which utilizes the key fact that the azimuthal variable along a spiral in the plane varies without limits. By applying an azimuth-scaling spiral transformation $\theta_2 = \theta_1/n$ as shown in Fig. 1, the phase of $n$ spiral turns in the input plane $(r_1, \theta_1)$ is mapped along one spiral turn in the output plane $(r_2, \theta_2)$, hence a vortex with inversely scaled charge $\ell_2 = n\ell_1$ is created, which is the key idea behind the proposed method. The concept works for either $|n| > 1$ or $|n| < 1$, without requiring $n$ to be an integer. Therefore, OAM multiplication or division by any rational factor can be achieved, which is a major difference from previous methods.

The proposed OAM multiplication and division scheme uses the following azimuth-scaling law, which is derived from an antianalytic complex mapping [39,42,43]

$$r_2 = c r_1^{-1/n}, \qquad \theta_2 = \theta_1/n, \tag{1}$$

where $c$ and $n$ are scaling factors. $(r_1, \theta_1)$ and $(r_2, \theta_2)$ are polar coordinates describing spirals in the input and output planes as shown in Fig. 1. The shape of the spirals is determined by functions in the form of $r = f(\theta)$, as for example $r = s\exp(a\theta)$ which represents logarithmic spirals ($s > 0$ is the radial position at $\theta = 0$ and $a$ is the exponential growth rate). This specific type of spirals is mapped through the above transformation to spirals in the output plane which are also logarithmic, namely

$$r_1 = s\exp(a\theta_1) \Rightarrow r_2 = c s^{-1/n}\exp(-a\theta_2). \tag{2}$$

The general case is examined in Sec. III of the Supplemental Material [39].

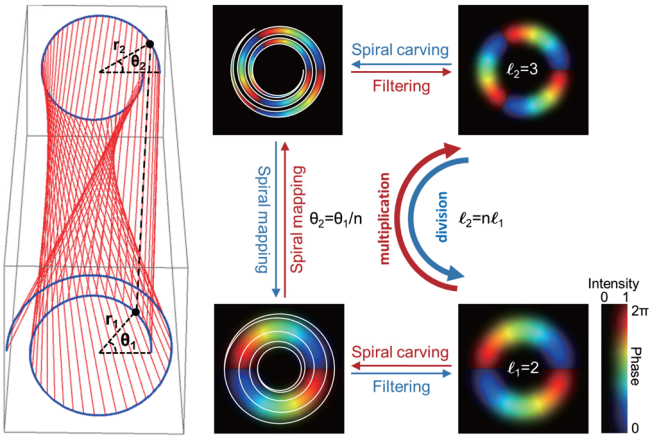


FIG. 1. The principle of OAM multiplication and division by an arbitrary rational factor with the proposed azimuth-scaling spiral transformation. A specific case of OAM multiplication with the scaling factor $n = 3/2$ and the inverse case of OAM division (multiplication by $n = 2/3$) are illustrated as an example. The input OAM wave front is carved into a spiral strip.

As the polar angle $\theta_1$ acts like a position parameter along the spiral, it varies continuously without limit. This is a fundamental difference between the proposed spiral transformation and the previous transformations (such as the log-polar or the circular-sector transformations), where $\theta_1$ is the standard polar angle varying along a $2\pi$ range. The unlimited range of the polar angle significantly extends the phase excursion that is available from the input OAM state, thus alleviating the need for the complex beam-copying or multitransformation diffractive stages that previous methods use in order to accomplish the desired $n$-fold increase of the phase. Moreover, the unlimited polar angle along a spiral can be arbitrarily compressed or decompressed, which allows our scheme to perform both OAM multiplication and division by any rational factor rather than only by integers. The advantages of the spiral transformation scheme come at the cost of an upper limit in power efficiency equal to $\min(|n|, |n|^{-1})$, which results from the fact that the spirals are unable to cover the whole area simultaneously in the input and output plane as shown in Fig. 1. In OAM multiplication ($|n| > 1$), the spiral strip in the input plane covers the entire beam area but is

transformed to an output spiral strip with dark gaps between its turns. As a result, the desired OAM coexists with a whole spectrum of OAM states and can only be isolated through low-pass spectral filtering at a power fraction of $|n|^{-1}$. In OAM division ($|n| < 1$), the output spiral strip covers the entire beam area, while the input spiral strip has gaps between its turns and utilizes at most a power fraction $|n|$ of the input OAM state [39].

In order to implement the proposed spiral transformation [Eq. (1)], a pair of phase masks are required, respectively, located in the input plane $(r_1, \theta_1)$ and output plane $(r_2, \theta_2)$, with a distance $d$ between the two parallel planes. The input phase mask (the *transformer*) has a phase modulation which is obtained by integrating the ray equations under the transformation Eq. (1) and is expressed as:

$$Q(r_1, \theta_1) = \frac{k}{d}\left[\frac{c r_1^q}{q}\cos(q\theta_1) - \frac{r_1^2}{2}\right], \tag{3}$$

where $k$ is the wave number and $q = 1 - n^{-1}$ for brevity. This is the phase modulation that has to be applied to the input OAM wave front within a defined spiral strip to redirect its constituent rays according to the spiral coordinate mapping [Eq. (1)]. Another phase mask (the *phase corrector*) is also required at the output plane to remove both phase $Q$ (only useful for the coordinate transformation) and the phase acquired during propagation:

$$P(r_2, \theta_2) = -Q(r_1, \theta_1) - k\sqrt{r_1^2 + r_2^2 - 2r_1 r_2 \cos(\theta_2 - \theta_1) + d^2}. \tag{4}$$

After the phase correction, the field $E_2$ at the output point $(r_2, \theta_2)$ is, within the context of ray optics, found to be equal to the field $E_1$ of the input OAM state $\exp(i\ell\theta_1)$ at the corresponding point $(r_1, \theta_1)$ multiplied by a simple mapping factor $\tau_{21} = -i\exp(ikd)|n|r_1/r_2$, which has a trivial constant phase part $-i\exp(ikd)$ and an amplitude part $|n|r_1/r_2$ resulting from $|E_1|^2|r_1 dr_1 d\theta_1| = |E_2|^2|r_2 dr_2 d\theta_2|$ imposed by the energy conservation. Therefore, the field at $(r_2, \theta_2)$ is proportional to $\exp(i\ell\theta_1) = \exp(in\ell\theta_2)$, which signifies an optical vortex with charge $n\ell$. A thorough analysis of the transformed field can be found in Secs. VI–VIII of [39].

The theoretical predictions of the spiral transformation scheme for arbitrary OAM multiplication or division have been verified by both simulation and experiment. Numerical simulations have been performed by computing the diffraction integral under an angular-spectrum decomposition of the fields, using perfect-vortex beams as input OAM states [39,44]. Typical values of the involved parameters in the simulation and the experiment are $d = 4.95$ mm, $\lambda_0 = 1550$ nm, $n_{\text{quartz}} = 1.444$, $k = 2\pi n_{\text{quartz}}/\lambda_0$, $a = \ln(1.2)/(2\pi)$ and $c = r_0^{1+1/n}$ with $r_0 = 340\ \mu$m $(n > 1)$, $r_0 = 280\ \mu$m $(n < -1)$, $r_0 = 320\ \mu$m $(0 < n < 1)$, $r_0 = 533\ \mu$m $(-1 < n < 0)$. For the experiment, an array of compact OAM multipliers and dividers with different scaling factors $n$ based on the above design are fabricated accordingly, as pairs of transmissive diffractive optical elements (DOEs) on the two opposite surfaces of a 4.95-mm-thick quartz plate as shown in Fig. 2(e). The enlarged images of the transformer and the phase-corrector DOEs are presented in Figs. 2(c) and 2(d) for the case $n = 3/2$, in comparison with the corresponding phase distributions given by Eqs. (3) and (4) (see Sec. X of [39] for all demonstrated cases). The devices are characterized using the optical setup as shown in Fig. 2(f). The right branch comprises a spatial light modulator (SLM) and a $4f$ system for producing the input OAM states. The lower branch includes the compact device and another $4f$ system with a pinhole in the intermediate Fourier plane for

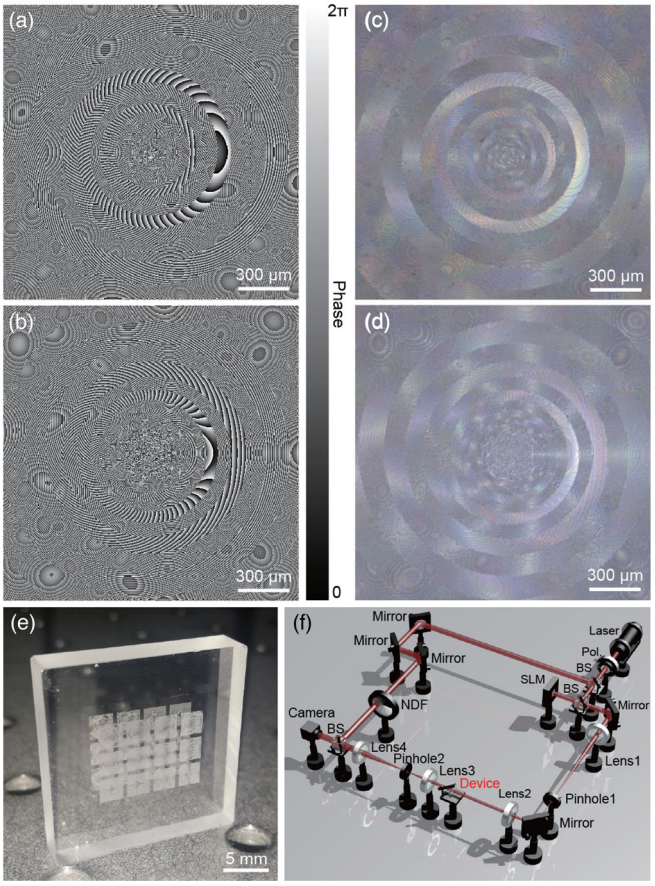


FIG. 2. Implementation of the proposed spiral transformation scheme for arbitrary OAM multiplication and division. (a), (b) Phase profiles and (c),(d) the corresponding fabricated diffractive optical elements of (a),(c) the transformer and (b), (d) the phase-corrector in the case of OAM multiplication with $n = 3/2$. (e) A $3 \times 4$ array of compact OAM multipliers and dividers with different factors $n$, whose transformers and phase correctors are fabricated on the two sides of a 4.95-mm-thick quartz plate. (f) Schematic of the optical setup for device characterization. Pol.: polarizer, BS: beam splitter, SLM: spatial light modulator, NDF: neutral density filter.

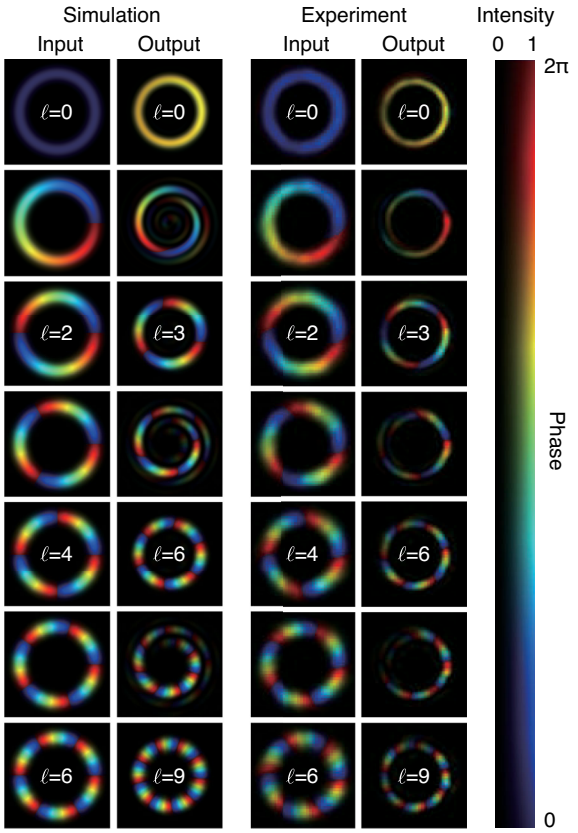


FIG. 3. Numerical and experimental intensity and phase distributions of the input and output OAM beams in the case of OAM multiplication with a factor $n = 3/2$. The experimental phase distributions were measured with quadrature phase-shift interference. The input vortex charges vary in $0 \leq \ell \leq 6$. All images have the same spatial scale.

low-pass spectral filtering. An infrared camera detects the final output beam. A reference Gaussian beam is available from the upper and left branch for interfering with the output beam through a beam splitter and revealing its phase structure based on a quadrature phase-shift interference method [45].

Figure 3 summarizes the numerical and experimental results of OAM multiplication with $n = 3/2$ for input OAM states with a fixed annular intensity and $0 \leq \ell \leq 6$. The final OAM states are obtained by low-pass spectral filtering of the output of the spiral transformation stage. The expected annular vortices with topological charge of $n\ell$ are obtained for the values of $\ell$ for which $n\ell$ is integer, namely $\ell = 0, 2, 4, 6$. For the other values of $\ell$, the filtering cannot isolate a single OAM state and the output contains a spectrum of (fractional) topological charges which give rise to azimuthal intensity variations, hence to a spiral intensity pattern [39,46,47]. Figure 4 shows the purity of the output integer OAM states in simulation and in experiment by performing angular Fourier transform on the output beams shown in Fig. 3. High mode purity is obtained for these OAM states with the side mode suppression ratio being

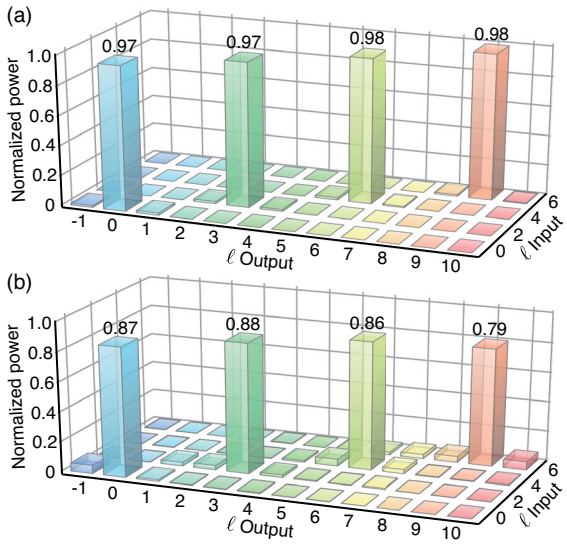


FIG. 4. OAM mode purity analysis of the output beams after OAM multiplication in Fig. 3. (a) Numerical and (b) experimental OAM spectra of the output beams.

higher than 18 dB in the simulation and 11.5 dB in the experiment. To the best of our knowledge, this is the first demonstration of OAM multiplication with a rational factor.

Further results that demonstrate the ability of the spiral transformation for OAM multiplication or division with

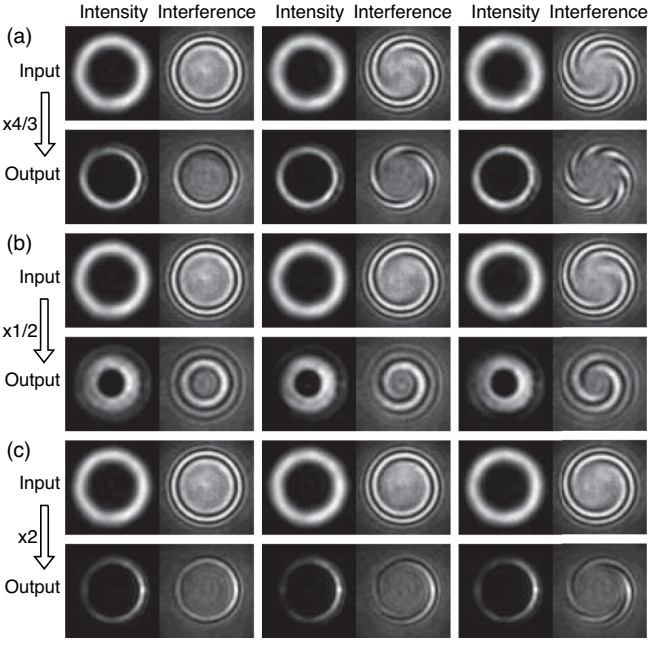


FIG. 5. Intensity and interference patterns of the input and output beams for OAM multiplication with factors (a) $n = 4/3$, (b) $n = 1/2$, and (c) $n = 2$. The topological charges can be inferred from the number of spiral arms in the interference patterns. For example, input $\ell = 0, 3, 6$ and output $\ell = 0, 4, 8$ in (a).

arbitrary factors are shown in Fig. 5 and in Sec. XII of [39]. Figure 5(b) shows a case of OAM division with $n = 1/2$. The vortex charges of the input and output beams are revealed as spiral arms in their interference patterns with a Gaussian beam. In all cases the expected OAM multiplication or division by the factor $n$ is verified. The measured power efficiencies also agree with the theoretical value $|n|^{-1}$ for all the $|n| > 1$ cases, which further confirms the theoretical predictions.

In summary, we have proposed a new optical transformation scheme for multiplying or dividing the OAM of light by an arbitrary rational factor. The key idea is that spirals in the transverse plane of an optical vortex offer an extended phase excursion which can be compressed or decompressed in the azimuthal direction with a single transformation to obtain an output state with correspondingly scaled OAM. The proposed scheme has particularly low complexity since it only involves a single transformation stage with two phase masks. Moreover, the same setup can perform both OAM multiplication and division by any rational factor, which is a significant improvement over previous schemes that use different techniques for multiplying or dividing OAM and the multiplication factor is limited to integer values. The performance of the azimuth-scaling spiral transformation has been verified by simulation as well as by experiment using homemade compact OAM multipliers and dividers. The advantages of the proposed scheme come at the cost of a basic limitation in power efficiency equal to $\min(|n|, |n|^{-1})$, which is similar to that of previous methods. A question for future research remains whether this limit can be surpassed while keeping the complexity of the setup reasonably low.

Being simple in implementation and able to perform both OAM multiplication and division by arbitrary rational factors, the proposed scheme may find applications within quantum as well as classical photonic information systems such as OAM-MDM communication systems, and in more fundamental studies of the OAM of light. The spiral transformations, as first demonstrated in high-resolution OAM mode sorting [28,29] and further through the present work, prove to be a powerful tool for manipulating the OAM of light. We envisage that further possibilities will open up in both the classical and the quantum regime if similar concepts are applied beyond standard quasiplanar optics such as in continuous transformation media and optical metamaterials.

This work is supported by the National Key R&D Program of China (Grants No. 2019YFA0706302 and No. 2018YFB1801800), National Natural Science Foundation of China (NSFC) (Grants No. U1701661, No. 11774437, No. 61975243, and No. 61490715), Local Innovative and Research Teams Project of Guangdong Pearl River Talents Program (Grant No. 2017BT01X121), Guangdong Basic and Applied Basic Research Foundation (Grant No. 2019A1515010858), and Science and Technology Program of Guangzhou (Grant No. 201804010302). Y. W. particularly thanks Shelly for the inspiration of this work.

*Corresponding author: chenyj69@mail.sysu.edu.cn
†Corresponding author: s.yu@bristol.ac.uk

[1] L. Allen, M. W. Beijersbergen, R. J. C. Spreeuw, and J. P. Woerdman, Orbital angular momentum of light and the transformation of Laguerre-Gaussian laser modes, Phys. Rev. A **45**, 8185 (1992).
[2] H. He, M. E. J. Friese, N. R. Heckenberg, and H. Rubinsztein-Dunlop, Direct Observation of Transfer of Angular Momentum to Absorptive Particles from a Laser Beam with a Phase Singularity, Phys. Rev. Lett. **75**, 826 (1995).
[3] N. B. Simpson, L. Allen, and M. J. Padgett, Optical tweezers and optical spanners with Laguerre-Gaussian modes, J. Mod. Opt. **43**, 2485 (1996).
[4] S. W. Hell and J. Wichmann, Breaking the diffraction resolution limit by stimulated emission: Stimulated-emission-depletion fluorescence microscopy, Opt. Lett. **19**, 780 (1994).
[5] S. Fürhapter, A. Jesacher, S. Bernet, and M. Ritsch-Marte, Spiral phase contrast imaging in microscopy, Opt. Express **13**, 689 (2005).
[6] G. Nienhuis, Doppler effect induced by rotating lenses, Opt. Commun. **132**, 8 (1996).
[7] J. Courtial, K. Dholakia, D. A. Robertson, L. Allen, and M. J. Padgett, Measurement of the Rotational Frequency Shift Imparted to a Rotating Light Beam Possessing Orbital Angular Momentum, Phys. Rev. Lett. **80**, 3217 (1998).
[8] G. Gibson, J. Courtial, M. J. Padgett, M. Vasnetsov, V. Pas'ko, S. M. Barnett, and S. Franke-Arnold, Free-space information transfer using light beams carrying orbital angular momentum, Opt. Express **12**, 5448 (2004).
[9] J. Wang, J.-Y. Yang, I. M. Fazal, N. Ahmed, Y. Yan, H. Huang, Y. Ren, Y. Yue, S. Dolinar, M. Tur, and A. E. Willner, Terabit free-space data transmission employing orbital angular momentum multiplexing, Nat. Photonics **6**, 488 (2012).
[10] N. Bozinovic, Y. Yue, Y. Ren, M. Tur, P. Kristensen, H. Huang, A. E. Willner, and S. Ramachandran, Terabit-scale orbital angular momentum mode division multiplexing in fibers, Science **340**, 1545 (2013).
[11] A. Mair, A. Vaziri, G. Weihs, and A. Zeilinger, Entanglement of the orbital angular momentum states of photons, Nature (London) **412**, 313 (2001).
[12] M. Bourennane, A. Karlsson, and G. Björk, Quantum key distribution using multilevel encoding, Phys. Rev. A **64**, 012306 (2001).
[13] A. Sit, F. Bouchard, R. Fickler, J. Gagnon-Bischoff, H. Larocque, K. Heshami, D. Elser, C. Peuntinger, K. Günthner, B. Heim, C. Marquardt, G. Leuchs, R. W. Boyd, and E. Karimi, High-dimensional intra-city quantum cryptography with structured photons, Optica **4**, 1006 (2017).
[14] N. R. Heckenberg, R. McDuff, C. P. Smith, and A. G. White, Generation of optical phase singularities by computer-generated holograms, Opt. Lett. **17**, 221 (1992).
[15] M. W. Beijersbergen, L. Allen, H. E. L. O. van der Veen, and J. P. Woerdman, Astigmatic laser mode converters and

transfer of orbital angular momentum, Opt. Commun. **96**, 123 (1993).
[16] M. W. Beijersbergen, R. P. C. Coerwinkel, M. Kristensen, and J. P. Woerdman, Helical-wavefront laser beams produced with a spiral phaseplate, Opt. Commun. **112**, 321 (1994).
[17] L. Marrucci, C. Manzo, and D. Paparo, Optical Spin-to-Orbital Angular Momentum Conversion in Inhomogeneous Anisotropic Media, Phys. Rev. Lett. **96**, 163905 (2006).
[18] X. Cai, J. Wang, M. J. Strain, B. Johnson-Morris, J. Zhu, M. Sorel, J. L. O'Brien, M. G. Thompson, and S. Yu, Integrated compact optical vortex beam emitters, Science **338**, 363 (2012).
[19] J. Leach, M. J. Padgett, S. M. Barnett, S. Franke-Arnold, and J. Courtial, Measuring the Orbital Angular Momentum of a Single Photon, Phys. Rev. Lett. **88**, 257901 (2002).
[20] Y. Zhou, M. Mirhosseini, D. Fu, J. Zhao, S. M. Hashemi Rafsanjani, A. E. Willner, and R. W. Boyd, Sorting Photons by Radial Quantum Number, Phys. Rev. Lett. **119**, 263602 (2017).
[21] N. Zhang, X. C. Yuan, and R. E. Burge, Extending the detection range of optical vortices by Dammann vortex gratings, Opt. Lett. **35**, 3495 (2010).
[22] G. Ruffato, M. Massari, and F. Romanato, Diffractive optics for combined spatial-and mode-division demultiplexing of optical vortices: Design, fabrication and optical characterization, Sci. Rep. **6**, 24760 (2016).
[23] T. Su, R. P. Scott, S. S. Djordjevic, N. K. Fontaine, D. J. Geisler, X. Cai, and S. J. B. Yoo, Demonstration of free space coherent optical communication using integrated silicon photonic orbital angular momentum devices, Opt. Express **20**, 9396 (2012).
[24] P. Bierdz, M. Kwon, C. Roncaioli, and H. Deng, High fidelity detection of the orbital angular momentum of light by time mapping, New J. Phys. **15**, 113062 (2013).
[25] G. Labroille, B. Denolle, P. Jian, P. Genevaux, N. Treps, and J.-F. Morizur, Efficient and mode selective spatial mode multiplexer based on multi-plane light conversion, Opt. Express **22**, 15599 (2014).
[26] G. C. G. Berkhout, M. P. J. Lavery, J. Courtial, M. W. Beijersbergen, and M. J. Padgett, Efficient Sorting of Orbital Angular Momentum States of Light, Phys. Rev. Lett. **105**, 153601 (2010).
[27] M. N. O'Sullivan, M. Mirhosseini, M. Malik, and R. W. Boyd, Near-perfect sorting of orbital angular momentum and angular position states of light, Opt. Express **20**, 24444 (2012).
[28] Y. Wen, I. Chremmos, Y. Chen, J. Zhu, Y. Zhang, and S. Yu, Spiral Transformation for High-Resolution and Efficient Sorting of Optical Vortex Modes, Phys. Rev. Lett. **120**, 193904 (2018).
[29] Y. Wen, I. Chremmos, Y. Chen, G. Zhu, J. Zhang, J. Zhu, Y. Zhang, J. Liu, and S. Yu, Compact and high-performance vortex mode sorter for multi-dimensional multiplexed fiber communication systems, Optica **7**, 254 (2020).
[30] Y. Yue, H. Huang, N. Ahmed, Y. Yan, Y. Ren, G. Xie, D. Rogawski, M. Tur, and A. E. Willner, Reconfigurable switching of orbital-angular-momentum-based free-space data channels, Opt. Lett. **38**, 5118 (2013).
[31] A. E. Willner, L. Li, G. Xie, Y. Ren, H. Huang, Y. Yue, N. Ahmed, M. J. Willner, A. J. Willner, Y. Yan, Z. Zhao, Z. Wang, C. Liu, M. Tur, and S. Ashrafi, Orbital-angular-momentum-based reconfigurable optical switching and routing, Photonics Res. **4**, B5 (2016).
[32] J. Liu and J. Wang, Demonstration of reconfigurable joint orbital angular momentum mode and space switching, Sci. Rep. **6**, 37331 (2016).
[33] A. Babazadeh, M. Erhard, F. Wang, M. Malik, R. Nouroozi, M. Krenn, and A. Zeilinger, High-Dimensional Single-Photon Quantum Gates: Concepts and Experiments, Phys. Rev. Lett. **119**, 180510 (2017).
[34] A. M. Steane, A tutorial on quantum error correction, in *Proceedings of the International School of Physics "Enrico Fermi," Course CLXII, Quantum Computers, Algorithms and Chaos* (IOS Press, Amsterdam, 2006), Vol. 162, pp. 1–24.
[35] W. J. Hossack, A. M. Darling, and A. Dahdouh, Coordinate transformations with multiple computer-generated optical elements, J. Mod. Opt. **34**, 1235 (1987).
[36] V. Potoček, F. M. Miatto, M. Mirhosseini, O. S. Magaña-Loaiza, A. C. Liapis, D. K. L. Oi, R. W. Boyd, and J. Jeffers, Quantum Hilbert Hotel, Phys. Rev. Lett. **115**, 160505 (2015).
[37] S. Takashima, H. Kobayashi, and K. Iwashita, Integer multiplier for the orbital angular momentum of light using a circular-sector transformation, Phys. Rev. A **100**, 063822 (2019).
[38] G. Ruffato, M. Massari, and F. Romanato, Multiplication and division of the orbital angular momentum of light with diffractive transformation optics, Light Sci. Appl. **8**, 113 (2019).
[39] See the Supplemental Material at http://link.aps.org/supplemental/10.1103/PhysRevLett.124.213901 for further analyses and results of OAM multiplication and division.
[40] Z. Zhao, Y. Ren, G. Xie, L. Li, Y. Yan, N. Ahmed, Z. Wang, C. Liu, A. J. Willner, S. Ashrafi, and A. E. Willner, Invited article: Division and multiplication of the state order for data-carrying orbital angular momentum beams, APL Photonics **1**, 090802 (2016).
[41] H. Zhou, J. Dong, J. Wang, S. Li, X. Cai, S. Yu, and X. Zhang, Orbital angular momentum divider of light, IEEE Photonics J. **9**, 1 (2017).
[42] J. Wang, *Semi-Analytic Function Conjugate Analytic Function* (Beijing University of Technology Press, Beijing, 1988).
[43] W. Appel, *Mathematics for Physics and Physicists* (Princeton University Press, Princeton, 2007).
[44] A. S. Ostrovsky, C. Rickenstorff-Parrao, and V. Arrizón, Generation of the "perfect" optical vortex using a liquid-crystal spatial light modulator, Opt. Lett. **38**, 534 (2013).
[45] G. Zhu, Y. Chen, Y. Liu, Y. Zhang, and S. Yu, Characterizing a $14 \times 14$ OAM mode transfer matrix of a ring-core fiber based on quadrature phase-shift interference, Opt. Lett. **42**, 1257 (2017).
[46] M. V. Berry, Optical vortices evolving from helicoidal integer and fractional phase steps, J. Opt. A **6**, 259 (2004).
[47] J. B. Götte, S. Franke-Arnold, R. Zambrini, and S. M. Barnett, Quantum formulation of fractional orbital angular momentum, J. Mod. Opt. **54**, 1723 (2007).